DOI: 10.1002/chem.200501214

Structural and Magnetic Studies of the Tris(cyclopentadienyl)manganese(II) "Paddle-Wheel" Anions $[Cp_{3-n}(MeCp)_nMn]^-$ ($n = 0$–3, $MeCp = C_5H_4CH_3$, $Cp = C_5H_5$)

Carmen Soria Alvarez,[a] Alan Bashall,[b] Eric J. L. McInnes,[c] Richard A. Layfield,*[a] Richard A. Mole,[a] Mary McPartlin,[b] Jeremy M. Rawson,*[a] Paul T. Wood,[a] and Dominic S. Wright*[a]

Abstract: The ion-contact complexes $[\{(\eta^5\text{-Cp})_2Mn(\eta^2{:}\eta^5\text{-Cp})K\}_3]\cdot 0.5\,THF$ (**1**·0.5 THF) and $[\{(\eta^2\text{-Cp})_2(\eta^2{:}\eta^5\text{-MeCp})MnK(thf)\}]\cdot 2\,THF$ (**2**·2 THF) and ion-separated complexes $[Mg(thf)_6][(\eta^2\text{-Cp})_3Mn]_2$ (**3**), $[Mg(thf)_6][(\eta^2\text{-Cp})(\eta^2\text{-MeCp})_2Mn)]_2\cdot 0.5\,THF$ (**4**·0.5 THF), $[Mg(thf)_6][(\eta^2\text{-MeCp})_3Mn)]_2\cdot 0.5\,THF$ (**5**·0.5 THF) and $[Li([12]crown\text{-}4)]_5[(\eta\text{-Cp})_3Mn]_5$ (**6**) ($Cp = C_5H_5$, $CpMe = C_5H_4CH_3$), have been prepared and structurally characterised. The effects of varying the Cp and CpMe ligands in complexes **1**–**5** have been probed by variable-temperature magnetic susceptibility measurements and EPR spectroscopic studies.

Keywords: cyclopentadienyl ligands · magnetic properties · manganese · structure elucidation

Introduction

The largely covalent character of the metal–ligand bonds within most d-block metallocenes stems from significant involvement of the valence d orbitals.[1] This situation contrasts with the minimal use (or even absence) of d orbitals in the metal–ligand bonding within main-group metallocenes, such as stannocene (Cp_2Sn), resulting in a significant polar/ionic character in these species.[2,3] The most notable exception to the trends found in d-block metallocene chemistry is manganocene, $[(Cp)_2Mn]$.[4] The antiferromagnetic behaviour of crystalline $[(Cp)_2Mn]$ in the temperature range 67–432 K strongly suggests predominantly ionic character for the metal–ligand interactions.[4] Subsequent work has confirmed these conclusions.[5] In contrast to the temperature-independent value of μ_{eff} for $[(Cp)_2Mn]$ in dilute hydrocarbon solution, solutions of dimethylmanganocene, $[(MeCp)_2Mn]$,[6] show a strongly temperature-dependent μ_{eff}. This behaviour has been attributed to a spin equilibrium between a high-spin $^6A_{1g}$ sextet state and a low-spin doublet state (either $^2E_{2g}$ or $^2A_{1g}$).[7]

The motivation for our work on manganese(II) cyclopentadienide complexes stems from a longstanding interest in the reactions of polar metallocenes with nucleophilic reagents. Group 14 metallocenes, Cp_2E (E = Sn, Pb), react with s-block metal cyclopentadienide reagents to furnish a homologous series of sandwich anions, $[(Cp)_{2n+1}E_n]^-[M(L)_x]^+$ (E = Sn, $n = 1$; E = Pb, $n = 1$, 2, 4; M = Li-Cs, L = crown ether or cryptand, $x = 1$–3).[2c] Also relevant are highly ionic, alkali metal cyclopentadienyl anions like $[(Cp)_2Li]^-$ and $[(Cp)_3Ba]^-$ reported by Harder and co-workers.[9] The extent of aggregation in these so-called "paddle-wheel" anions (i.e., the value of n) is governed by the stoichiometry of the reagents and the thermochemical radius of the counterion (i.e., the nature of the co-solvent, L, and the value of x). The latter signifies the importance of lattice energies in determining the outcomes of the reactions. The

[a] Dr. C. S. Alvarez, Dr. R. A. Layfield, R. A. Mole, Dr. J. M. Rawson, Dr. P. T. Wood, Dr. D. S. Wright
University of Cambridge, Department of Chemistry
Lensfield Road, Cambridge, CB2 1EW (UK)
Fax: (+44) 1223-336-362
E-mail: ral34@cam.ac.uk
jmr31@cam.ac.uk
dsw1000@cus.cam.ac.uk

[b] Dr. A. Bashall, Prof. M. McPartlin
School of Chemistry, London Metropolitan University
Holloway Road, London N7 8DB (UK)

[c] Dr. E. J. L. McInnes
Department of Chemistry, The University of Manchester
Oxford Road, Manchester M13 9PL (UK)

Supporting information for this article is available on the WWW under http://www.chemeurj.org/ or from the author.

predominantly ionic character of manganocenes makes them ideal candidates for extension of our earlier work on p-block metallocenes to paramagnetic, d-block counterparts. In a recent communication we described the syntheses, structures and magnetic properties of $[(\eta^2\text{-Cp})_2\text{Mn}(\eta^2{:}\eta^5\text{-Cp})\text{K}]\cdot 0.5\,\text{THF}$ (**1**·0.5 THF) and $[\text{Mg(thf)}_6][(\eta^2\text{-Cp})_3\text{Mn}]_2$ (**3**), the first reported examples of the $[\text{Cp}_3\text{Mn}]^-$ ion.[9] Independently of our work, the structures of $[\text{Cs}([18]\text{crown-6})_2][(\eta^2\text{-Cp})_3\text{Mn}]$, $[\text{Cs}([18]\text{crown-6})_2][(\eta^2\text{-MeCp})_3\text{Mn}]$ and $[\text{Cs}\{(\eta^2\text{-Cp})_3\text{Mn}\}]$ were also reported.[10] The significance of the adoption of tris(η^2-Cp) bonding in all of these species and the extent to which steric, electronic or lattice effects play a role is not evident, although calculations suggest that the ligand bonding mode in this type of anion is likely to be highly flexible.[10]

We report here a full account of our studies in this area which addresses two issues, 1) the factor(s) involved in ligand–Mn bonding in triscyclopentadienyl manganese anions and 2) the possibility of tuning the magnetic properties of these species by ligand substitution. The syntheses and structures of the new paddle-wheel complexes $[(\eta^2\text{-Cp})_2\text{Mn}(\eta^2{:}\eta^5\text{-MeCp})\text{K}]\cdot 2\,\text{THF}$ (**2**·2 THF), $[\text{Mg(thf)}_6][(\eta^2\text{-Cp})(\eta^2\text{-MeCp})_2\text{Mn})]_2\cdot 0.5\,\text{THF}$ (**4**·0.5 THF), $[\text{Mg(thf)}_6][(\eta^2\text{-MeCp})_3\text{Mn})]_2\cdot 0.5\text{THF}$ (**5**·0.5 THF), and $[\text{Li}([12]\text{crown-4})]_5[(\eta\text{-Cp})_3\text{Mn}]_5$ (**6**), together with variable-temperature magnetic susceptibility studies and EPR spectroscopic studies of compounds **1**–**5** are reported. Although all previous compounds have contained three η^2-bonded cyclopentadienyl ligands, the observation of three distinct bonding arrangements for the $[(\eta\text{-Cp})_3\text{Mn}]^-$ ions in **6** (involving combinations of η^2-, η^3- and η^5-ligand bonding) provides the first experimental evidence for the flexibility of Cp–metal bonding in triscyclopentadienyl manganocene anions and emphasises the fact that there is no electronic significance in the formal 14 e count observed in the tris-η^2-ligand arrangement.

Results and Discussion

The new complexes $[(\eta^2\text{-Cp})_2\text{Mn}(\eta^2{:}\eta^5\text{-MeCp})\text{K}]\cdot 2\,\text{THF}$ (**2**·2 THF), $[\text{Mg(thf)}_6][(\eta^2\text{-Cp})(\eta^2\text{-MeCp})_2\text{Mn}]_2\cdot 0.5\,\text{THF}$ (**4**·0.5 THF), $[\text{Mg(thf)}_6][(\eta^2\text{-MeCp})_3\text{Mn})]_2\cdot 0.5\,\text{THF}$ (**5**·0.5 THF) and $[\text{Li}([12]\text{crown-4})_2]_5[(\eta\text{-Cp})_3\text{Mn}]_5$ (**6**) and the previously reported complexes $[\{(\eta^5\text{-Cp})_2\text{Mn}(\eta^2{:}\eta^5\text{-Cp})\text{K}\}_3]\cdot 0.5\,\text{THF}$ (**1**·0.5 THF) and $[\text{Mg(thf)}_6][(\eta^2\text{-Cp})_3\text{Mn}]_2$ (**3**)[9] were prepared according to Schemes 1 and 2 (in yields of 17–52%). Complex **6** was obtained reproducibly in low yield (ca. 1%) from the 2:1 reaction of $[(\text{Cp})_2\text{Mn}]$ with CpLi in the presence of [12]crown-4 (two equivalents). The aim of this reaction was to obtain $[(\text{Cp})_5\text{Mn}_2][\text{Li}([12]\text{crown-4})_2]$ (**7**), containing the dinuclear Mn^{II} homologue of the $[(\text{Cp})_3\text{Mn}]^-$ ion $[(\text{Cp})_2\text{Mn}(\mu\text{-Cp})\text{Mn}(\text{Cp})_2]^-$ (analogous to the previously reported $[(\text{Cp})_2\text{Pb}(\mu\text{-Cp})\text{Pb}(\text{Cp})_2]^-$ ion which was prepared by a similar route from $[(\text{Cp})_2\text{Pb}]$[11]; (Scheme 3). Owing to the low yield of **6**, it could only be characterised by X-ray crystallography. Later structural characterisation of **6** showed that the complex contains mononuclear $[\text{Cp}_3\text{Mn}]^-$ ions (similar to those in **1**–**5**).

$$[(\text{Cp})_2\text{Mn}] + \text{Cp'K} \xrightarrow{\text{THF}} [\{(\eta^2\text{-Cp})_2\text{Mn}(\eta^2{:}\eta^5\text{-Cp'})\text{K(thf)}\}\cdot n\text{THF}]$$

Cp' = Cp, $n = 0.5$, **1**
Cp' = MeCp, $n = 2$, **2**

Scheme 1.

$$2[(\text{Cp'})_2\text{Mn}] + [(\text{Cp''})_2\text{Mg}] \xrightarrow{\text{THF}} [(\eta^2\text{-Cp'})_n(\eta^2\text{-Cp''})_{3-n}\text{Mn}]_2[\text{Mg(thf)}_6]\cdot x(\text{THF})$$

$n = 3$, Cp' = Cp'' = Cp, $x = 2$, **3**
$n = 1$, Cp' = Cp, Cp'' = MeCp, $x = 0$, **4**
$n = 0$, Cp' = Cp'' = MeCp, $x = 0.5$, **5**

Scheme 2.

$$2[(\text{Cp})_2\text{Mn}] + \text{CpLi} \xrightarrow{\text{THF/[12]crown-4}} \begin{cases} [\text{Cp}_2\text{Mn}(\mu\text{-Cp})\text{MnCp}_2][\text{Li}([12]\text{crown-4})_2] & \textbf{7} \\ [\text{Cp}_3\text{Mn}][\text{Li}([12]\text{crown-4})_2] & \textbf{6} \end{cases}$$

Scheme 3.

Complexes **2**, **4**, **5** and **6** are very air-sensitive in solution and the solid state (dried crystals of **2** are pyrophoric). For the CpMe complexes **2**, **4** and **5**, the rate of decomposition in air was observed to increase with increasing methyl substitution, this is consistent with observations on the parent compounds $[(\text{Cp})_2\text{Mn}]$ and $[(\text{MeCp})_2\text{Mn}]$.[4a,6] Whereas **2** and **6** are stable indefinitely at room temperature under dinitrogen or argon, complexes **4** and **5** decompose over a period of approximately two weeks. All the complexes are moderately soluble in polar solvents (e.g., THF, DMSO), but insoluble in hydrocarbon solvents. The extreme air-sensitivity of complexes **2**, **4** and **5** and the presence of labile, lattice-bound THF molecules in their crystalline solvates meant that reproducible elemental analysis was difficult to obtain. However, satisfactory analyses were obtained on all of these compounds after repeated attempts. The results are consistent with the removal of lattice-bound THF on drying the compounds in vacuo for about 30 minutes [10^{-1} atm (100 mbar)] prior to isolation. The number of lattice-bound THF molecules in crystalline **2**·THF, **4**·0.5 THF and **5**·0.5 THF was determined by subsequent X-ray crystallographic studies (see later discussion). In the case of **6**, satisfactory elemental analysis could not be obtained and its characterisation was made only on the basis of spectroscopic and X-ray analysis. Although resonances due to the Cp ring protons could be assigned for each complex ($\delta(^1\text{H})$ **2**: 5.60; **4**: 9.25; **5**: 9.35 ppm), no detailed information concerning the solution-phase structures of **2**, **4**, **5** and **6** could be discerned from NMR spectroscopy due to the presence of very broad resonances arising from their paramagnetism. The IR spectra of **2**, **4** and **5** confirm the presence of the Cp ligands through their characteristic sp^2 C–H stretching bands (**2**:

3059; **4**: 3066; **5**: 3066 cm^{-1}), and also the presence of the THF or [12]crown-4 ligands from the C–O stretching bands (**2**: 1011; **4**: 1011; **5**: 1012 cm^{-1}).

The low-temperature (180 K) X-ray structures of the new compounds **2**·2THF, **4**·0.5THF, **5**·0.5THF and **6** were obtained. Selected bond lengths and angles for the ion-paired complex **2**·2THF are shown in Table 1. Table 2 contains the Mn–C bond lengths found in **2**·2THF, **4**·0.5THF and **5**·0.5THF as well as those found in the previously reported complexes **1**·0.5THF and **3** for comparison, and Table 3 lists the Mn–C distances found in compound **6**. Details of the data collections and refinements of **2**·2THF, **4**·0.5THF, **5**·0.5THF and **6** are given in the Experimental Section.

Table 1. Selected mean bond lengths [Å] and angles [°] for complex **2**.

Mn(1)–C(1,1′)	2.36(1)	K(1,1′)–C(1,2′)	3.24(1)
Mn(1)–C(2,2′)	2.38(1)	K(1,1′)–C(2,1′)	3.09(1)
Mn(1)···C(3,3′)	2.92(1)	K(1,1′)–C(3,5′)	3.05(1)
Mn(1)···C(4,4′)	3.18(1)	K(1,1′)–C(4,4′)	3.18(1)
Mn(1)···C(5,5′)	2.88(1)	K(1,1′)–C(5,3′)	3.30(1)
K(1,1′)···Cp_c	2.94		
Cp_c-K(1,1′)-Cp_c(A)	117.6(1)	Cp_c-Mn(1)-Cp_c	119.8(1).

Complex **2**·2THF crystallizes in the space group $P6_3$ with formulation $[(\eta^2\text{-Cp})_2Mn(\eta^2{:}\eta^5\text{-MeCp})K(thf)]\cdot 0.5\,THF$. There is extensive disorder of the Cp/CpMe and THF ligands, as well as the K^+ ions. In the asymmetric unit of **2** the manganese atom lies on an axis of C_3 symmetry (Figure 1, Table 1), being bonded in a η^2-mode to one unique cyclopentadienyl ring, which is 50:50 disordered, giving two independent rings of half occupancy. The Mn^{II} centre is therefore coordinated by three symmetry related η^2-Cp ligands in a "paddle-wheel" arrangement to create an approximately trigonal planar coordination geometry at manganese atom, with the Mn atom itself lying out of the plane of the midpoints of the three η^2-(C–C) bonds. Symmetry-related η^5-bridging interactions to symmetry-related K^+ ions are responsible for the association of the $[(\eta^2\text{-Cp})_2Mn(\eta^2{:}\eta^5\text{-MeCp})K]^-$ units into the infinite polymeric hexagonal layers shown in Figure 2. The Mn centres in each layer are exactly coplanar by symmetry. The disorder of the Cp rings arises from a random distribution throughout the crystal of hexagonal layers of opposite chirality, and there is a corresponding 50:50 disorder of the K^+ ion (K(1) and K(1′)) bonding in the η^5-mode to the two orientations of the Cp ring and of the oxygen donor atom of the coordinated THF ligand (O(1) and O(1′)). The metric parameters in the two disordered components of the complex

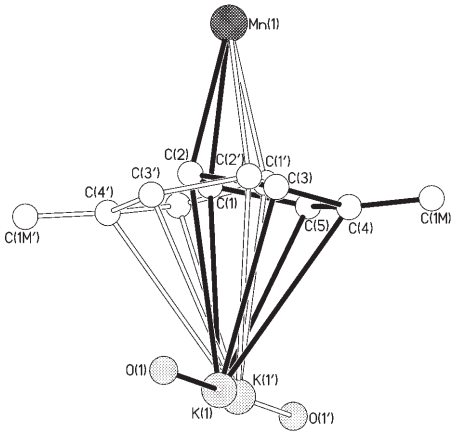

Figure 1. The asymmetric unit of **2** showing the disordered Cp ligand and K atom. Hydrogen atoms are omitted for clarity.

Table 2. Comparison of the bond lengths [Å] in the $[Cp_3Mn]^-$ ions **1**·0.5THF, **2**·2THF (mean values), **3**, **4**·0.5THF and **5**·0.5THF.

	1[a]	**2**	**3**[a]	**4**	**5**
Mn(1)–C(1)	2.392(5)	2.36(1)	2.360(5)	2.311(4)	2.346(8)
Mn(1)–C(2)	2.364(6)	2.38(1)	2.351(6)	2.371(4)	2.379(8)
Mn(1)–C(3)	2.86(4)	2.92(1)	2.823(6)	2.953(5)	2.953(8)
Mn(1)–C(4)	3.15(5)	3.18(1)	3.157(6)	3.227(6)	3.213(8)
Mn(1)–C(5)	2.90(2)	2.88(1)	2.853(6)	2.885(6)	2.895(8)

[a] From reference [9].

Table 3. Bond lengths (Mn–C) [Å] for compound **6**.

	$3\eta^2$	$3\eta^2$	$2\eta^2\eta^3$	$2\eta^2\eta^3$	$2\eta^2\eta^5$
C(11)	2.425(6)	2.345(6)	2.338(7)	2.413(6)	2.454(6)
C(12)	2.339(6)	2.429(6)	2.356(7)	2.376(7)	2.421(6)
C(13)	2.893	2.820	2.811	2.974	2.970
C(14)	3.282	2.951	3.081	3.256	3.274
C(15)	3.028	2.682	2.808	2.985	3.006
C(21)	2.390(7)	2.412(6)	2.469(7)	2.361(5)	2.390(6)
C(22)	2.373(6)	2.444(6)	2.409(7)	2.403(5)	2.413(5)
C(23)	2.933	3.246	3.114	3.102	3.180
C(24)	3.256	3.624	3.508	3.446	3.570
C(25)	2.989	3.624	3.203	3.056	3.165
C(31)	2.312(6)	2.443(5)	2.474(8)	2.479(6)	2.404(7)
C(32)	2.443(6)	2.309(5)	2.432(9)	2.355(5)	2.413(7)
C(33)	2.886	2.552(5)	2.551(8)	2.453(5)	2.506(7)
C(34)	2.985	2.820	2.743	2.669	2.561(7)
C(35)	2.696	2.756	2.656	2.681	2.469(7)

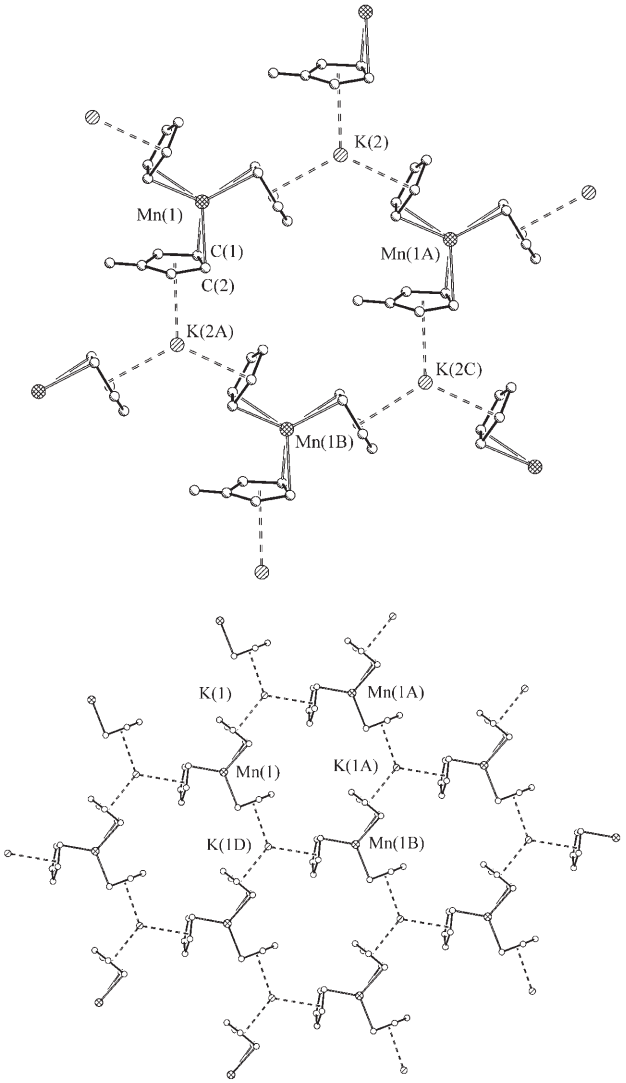

Figure 2. A hexagonal unit in the crystal structure of **2** showing the mode of propagation throughout the lattice (top), and a segment of the layered structure of **1** (bottom). Hydrogen atoms and disordered THF molecules omitted for clarity.

are equal within experimental error and mean values will mainly be used in the discussion.

The mean planes of the C_5H_5 ring in **2** are nearly perpendicular to the plane of the Mn centres, but slightly tipped in opposite directions (dihedral angles 88° C(1–5) and 93° C(1′–5′)). The Mn(1)–C(1) and Mn(1)–C(2) bond lengths are 2.36(1) Å and 2.38(1) Å, respectively, with the remaining Mn(1)–C(3–5) distances (2.88(1)–3.18(1) Å) being too long to be indicative of bonding. The Me groups of the CpMe ligands are located furthermost from the manganese centre (Mn(4)–C(4) 3.18(1)). The K(1)–C(1–5) distances are in the range 3.05(1)–3.33(1) Å, corresponding to approximate η^5-coordination of the Cp ligand. Each K^+ centre is additionally coordinated by one THF ligand, with a mean K–O(1) distance of 2.91(3) Å (average K–O distance 2.822 Å, range 2.264–3.933 Å[12]). The K–O bond vector is perpendicular to the plane of the Mn^{II} centres and there are 0.5 molecules of lattice-bound THF per asymmetric unit. The overall crystal structures of **1**·0.5 THF and **2**·2 THF are very similar, with the asymmetric units in each associating into hexagonal rings in which manganese and potassium cations alternate at the corners.[9]

The Mn^{2+} ions in the honeycomb layers are coplanar. Adjacent layers are offset in a manner similar to that observed in the extended ABAB-type structure of graphite, such that the K^+ centres in neighbouring layers are eclipsed and the Mn^{2+} ions staggered. The interlayer separations in both **1**·0.5 THF[9] and **2**·2 THF are very large at approximately 9.53 Å (corresponding to the perpendicular mean plane separation between adjacent layers); the large volume between the layers being only partially occupied by the coordinated and lattice-bound THF molecules.

Molecules of **4** crystallize in the rhombohedral space group $R\bar{3}c$. The asymmetric unit $[Mg(thf)_6][(\eta^2\text{-Cp})(\eta^2\text{-MeCp})_2Mn]_2$ is composed of two discrete $[(\eta^2\text{-Cp})(\eta^2\text{-MeCp})_2Mn]^-$ paddle-wheel ions and an octahedral $[Mg(thf)_6]^{2+}$ ion (Figure 3).

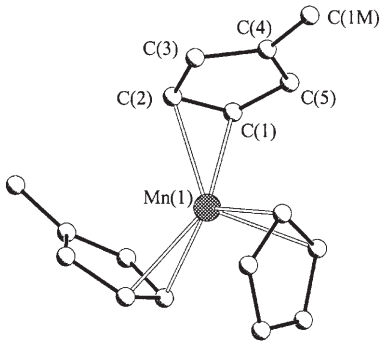

Figure 3. The molecular structure of one $[(\eta^2\text{-Cp})(\eta^2\text{-MeCp})_2Mn]^-$ ion of **4** (hydrogen atoms omitted for clarity).

The Mn-C(η^2-Cp) distances in **4**·0.5 THF fall in the range 2.311(4)–2.371(4) Å (Table 3). The CH_3 substituents on the MeCp ligands are coplanar with the pseudo-trigonal plane of the $[(\eta^2\text{-Cp}')_3Mn]^-$ ions and are related by symmetry about the pseudo-threefold rotation axis of these anions. The mirror plane coincident with this pseudo-trigonal plane gives the $[(\eta^2\text{-Cp})(\eta^2\text{-MeCp})_2Mn]^-$ ion molecular C_s symmetry. The structure of the complex $[(\eta^2\text{-MeCp})_3Mn]_2[Mg(thf)_6]$·0.5 THF (**5**·0.5 THF) similarly consists of discrete $[(\eta^2\text{-MeCp})_3Mn]^-$ and $[Mg(thf)_6]^{2+}$ ions (Figure 4). The Mn–C(η^2-Cp) distances in the range 2.346(8)–2.379(8) Å (Table 3) are very similar to those in **1**–**4**, and the individual anions of **5** possess C_{3h} point symmetry, since the carbon atoms of the methyl groups are coplanar with manganese. The $[Mg(thf)_6]^{2+}$ ion in **5** is isomorphous with that in **4**. It is worth mentioning that the structures of **2** and **4** contain the first examples of heteroleptic triscyclopentadienyl anions.[9,10]

The unexpected formation of $[Li([12]crown\text{-}4)_2]_5[(\eta\text{-Cp})_3Mn]_5$ (**6**) was revealed by low-temperature X-ray crys-

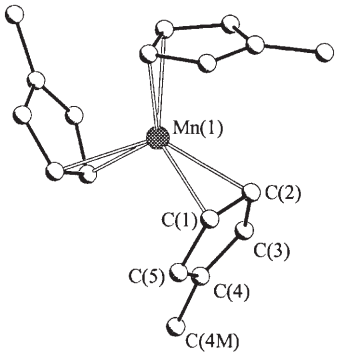

Figure 4. The molecular structure of one $[(\eta^2\text{-MeCp})_3Mn]^-$ ion of **5** (hydrogen atoms omitted for clarity).

tallography, and showed the presence of five unique $[(\eta\text{-Cp})_3Mn]^-$ ions in the unit cell, distinguishable by varying Cp hapticities of η^2-, η^3- or η^5- (Figure 5).

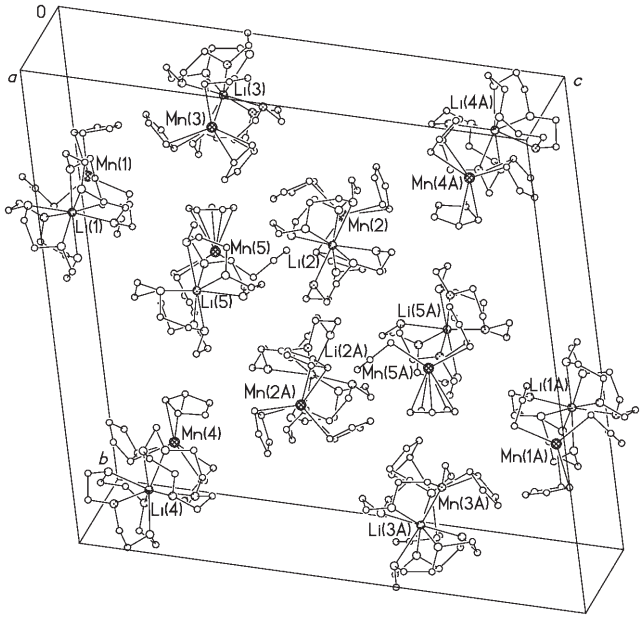

Figure 5. The unit cell of **6**. The disorder in the $[Li([12]crown\text{-}4)_2]^+$ ions is not shown for clarity.

The $[(\eta^2\text{-Cp})_3Mn]^-$ coordination mode observed in the anions of **1–5** and in the other reported complexes of this type, for example, $[(\eta^2\text{-Cp})_3Mn][Cs([18]crown\text{-}6)_2]$, $[(\eta^2\text{-MeCp})_3Mn][Cs([18]crown\text{-}6)_2]$ and $[Cs\{(\eta^2\text{-Cp})_3Mn\}]$,[10] is only seen in two anions within the unit cell of **6** (i.e., Mn(1)). The coordination mode adopted at Mn(2), Mn(3) and Mn(4) is $2\eta^2\eta^3$, whilst at Mn(5) a $2\eta^2\eta^5$ bonding arrangement is observed. These coordination modes are unique, having never been observed previously in any $[(Cp)_3Mn]^-$ complex. The Mn–C bond distances of 2.309(5)–2.561(7) Åin the five unique anions of **6** all fall within in the range expected for an ionic (high-spin) manganocene[12] and the range of Mn–C distances narrows with decreasing total hapticity (Table 3). The $[Li([12]crown\text{-}4)_2]^+$ ions of **6** exhibit site disorder.

The observation of three different types of anion in the structure of **6** is of interest in regard to previous DFT calculations of $[Cp_3Mn]^-$ containing different hapticities of the Cp ligands.[10] This study considered six $[Cp_3Mn]^-$ ions in which the ligand hapticities were $3\eta^2$, $3\eta^1$, $2\eta^1\eta^5$, $2\eta^2\eta^1$, $\eta^1\eta^2\eta^5$, $2\eta^2\eta^5$, but the $\eta^2\eta^2\eta^3$ arrangement observed in the structure of **6** was not considered. The main conclusions from this study were that the $3\eta^2$ coordination mode was the most stable arrangement and that a spin density of 5α (i.e., high-spin) on manganese was generally lower in energy than the low-spin configurations (for which convergence could be obtained). The structure of **6** is in broad agreement with the previous theoretical study insofar as it confirms that the energies of the various bonding modes are well within the upper limit normally exerted by crystal packing forces, the energy separations of the various alternatives being in the range 0–7 $kJ\,mol^{-1}$. This means that the bonding alternatives should be dominated by the energetics of the bulk lattice.[13] Although the individual spin states of the anions in the structure of **6** would be impossible to identify by magnetic measurements of bulk samples of the complex, each $[Cp_3Mn]^-$ ion would be expected to be high-spin on the basis of the Mn–C bond lengths, which all fall within the range expected for a high-spin manganese cyclopentadienide ($S=5/2$). This is also consistent with the calculations on the model structures previously reported.

Physical measurements: The magnetic behaviour of manganocenes has been the subject of some debate.[5b,6,7,14] Experimental studies have indicated that the value of χT (or μ_{eff}) decreases on cooling. Initial studies on $[(Cp)_2Mn]$ and $[(CpMe)_2Mn]$ suggested that the reduction in χT could be attributed to antiferromagnetic interactions between ions.[6] However, EPR studies in dilute solution (in which intermolecular effects might be considered negligible) suggested that this assignment might be erroneous and that the behaviour of manganocenes might be more appropriately ascribed to a high-spin/low-spin equilibrium.[5b] Further studies on dilute solutions of $[(Cp)_2Mn]$ in toluene by using the Evans method were consistent with a $^2E_{2g}$ low-spin ground state and a thermodynamically accessible $^6A_{1g}$ high-spin excited state. Temperature-dependent studies by Rettig and coworkers[7a] indicated the thermodynamic properties associated with the high-spin/low-spin equilibrium constant K for $[(CpMe)_2Mn]$ are $\Delta H=7531\,J\,mol^{-1}$ and $\Delta S=24.3\,J\,K^{-1}\,mol^{-1}$. Their analysis of Wilkinson's data[7a] for $[(Cp)_2Mn]$ in the molten state indicated similar behaviour ($\Delta H=8500\,J\,mol^{-1}$, $\Delta S=29.5\,J\,K^{-1}\,mol^{-1}$). Since the original and extensive studies on $[(Cp)_2Mn]$ and $[(CpMe)_2Mn]$, there have been few additional studies on high-spin/low-spin equilibria in manganocene derivatives.[8,9] We have studied the electronic properties of the current series of manganocene anions through variable-temperature EPR spectroscopy and SQUID magnetometry.

EPR studies: Previous X-band EPR studies by Voitlander et al. on crystals of $[(Cp)_2Mn]$ and $[(Cp)_2Mn]$ doped into

$[(Cp)_2Mg]$[14] revealed single resonances with g values close to the spin-only value of 2.0. The lack of additional structure was ascribed to combinations of either exchange averaging of the hyperfine structure, or observation of only the $-{}^1/_2 \rightarrow +{}^1/_2$ transition due to a large zero-field splitting. Previous low-temperature solution studies on dilute samples of high-spin $[(Cp)_2Mn]$ in $[(Cp)_2Mg]$ and low-spin $[(CpMe)_2Mn]$ in $[(CpMe)_2Mg]$ indicate ^{55}Mn hyperfine interactions (<100 G at X-band) that are certainly less than the linewidth at Q-band. Notably, the resolution of this hyperfine coupling ($<7\times10^{-3}$ cm^{-1}~75 G) even in these magnetically dilute systems was strongly temperature dependent and usually became unobservable above 77 K.[7b] In addition, subsequent studies by Rettig and co-workers at Q-band[7a] identified additional resonances near zero-field indicative of large zero-field splittings for Mn^{2+} ($D\sim0.5$ cm^{-1}). These two factors coupled with the possibility of additional dipolar line broadening in these magnetically concentrated systems are likely to mask any ^{55}Mn hyperfine coupling in the current studies.

Solid-state EPR spectra of polycrystalline samples of **1**, **2**, **4** and **5** were recorded between 5 K and 300 K at Q-band (~34 GHz). All compounds exhibit similar EPR spectra. At room temperature a broad (ΔH_{pp}~220–300 G) single resonance at $g=1.956$ is typically observed (Figure 6) with no

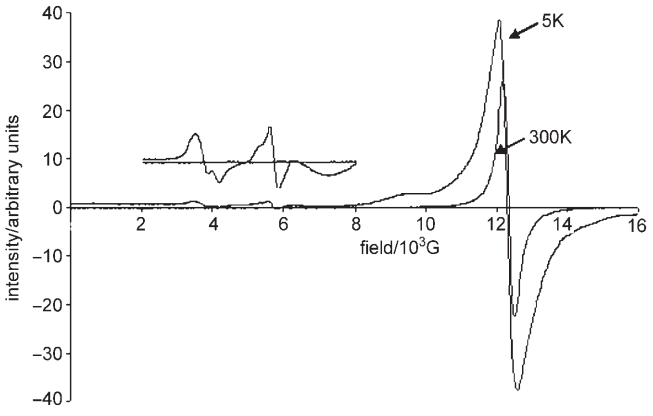

Figure 6. The Q-band powder EPR spectrum of **3** at 300 K and 5 K. The region 2000–8000G is expanded.

observable hyperfine coupling. For **1**–**5** the peak-to-peak linewidth (ΔH_{pp}) of the EPR resonance remains approximately constant down to 70 K (Figure 7). For **2** and **4** notable increases in linewidth are observed on cooling below 70 K and for all four derivatives an abrupt increase in linewidth is observed on cooling below 20 K (Figure 7). The general line broadness is likely to arise out of dipolar exchange coupling between Mn centres.

On cooling, additional low intensity transitions become detected at approximately 3.7 and 5.7 kG at Q-band, and a prominent shoulder at approximately 9.5 kG becomes resolved. These additional features might be attributable to zero-field splitting effects at Mn^{II}. However there is no clear evidence for the presence of the low-spin doublet state in any of the studies undertaken here.

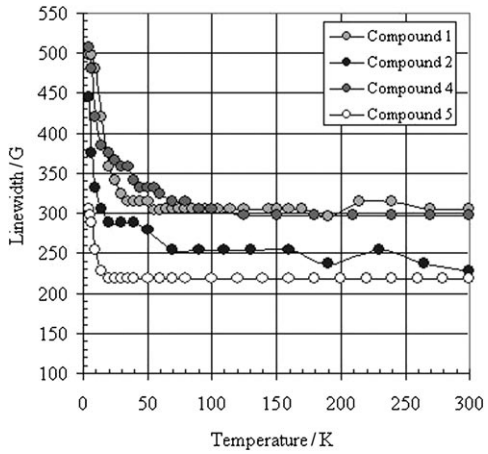

Figure 7. Temperature dependence of the peak-to-peak linewidth (ΔH_{pp}) of the Q-band EPR spectrum for compounds **1**, **2**, **4** and **5**.

Magnetic measurements: Magneto–structural correlations allow us to rationalise the susceptibility behaviour of this series of cyclopentadienyl and methylcyclopentadienyl manganese compounds. The large Mn–Mn distances and the evidence for mainly ionic bonding would indicate that any interaction between the nearest neighbour ions would be weak and dipolar in origin. We will therefore treat the Mn^{II} ions as well-isolated spins. The environment of each Mn ion is approximately C_{3v}, for which the predicted d-orbital splitting is shown in Figure 8. The five d electrons can populate

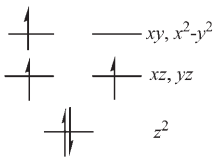

Figure 8. A d-orbital splitting diagram for trigonal planar geometry. The arrangement of electrons is that suggested for the magnetic ground state.

these to give a net $S={}^1/_2$, ${}^3/_2$, or ${}^5/_2$ spin on each ion. The predicted Curie constants [Eq. (1)] for these spin states are 0.375, 1.876 and 4.377 cm^3 K mol^{-1}, respectively. The presence of an $S={}^1/_2$ doublet ground state can be precluded on the basis of the EPR spectra, though this technique was unable to distinguish between the presence of the $S={}^3/_2$ or ${}^5/_2$ spin states.

$$\chi = \frac{Ng^2\beta^2S(S+1)}{3kT} = \frac{C}{T-\Theta}$$

The susceptibility data for compounds **1**–**5** was obtained between 5–300 K. All samples show Curie–Weiss behaviour [Eq. (1)] in the high-temperature regime as expected (illustrated for complex **1** in Figure 9; a graph of the behaviour of all of the complexes can be found in the Supporting Information). In all cases the value of χT initially decreases with falling temperature. The linewidths of the EPR spectra also increase significantly upon cooling to low temperature;

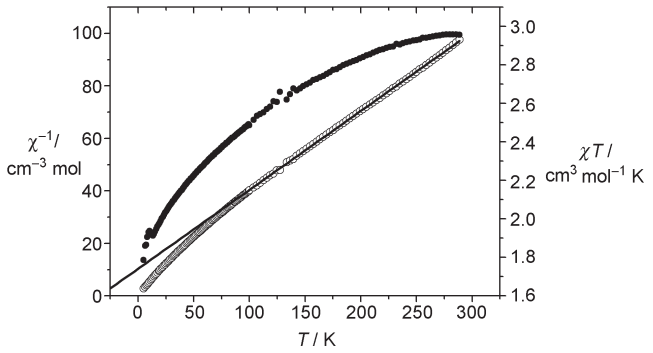

Figure 9. Graph of χT versus T and χ versus T for compound **1** including a fit to the Curie–Weiss law.

this result may in part be ascribed to the effect of very weak dipolar interactions.[15] However, EPR spectroscopy is very sensitive to even weak dipolar coupling, and these interactions will be too small to account for the observed decrease in χT alone. The observed Curie constants are shown in Table 4. These values are in agreement with the EPR data

Table 4. Curie-Weiss behaviour for **1**–**5** (esds are in parenthesis).

	1	**2**	**3**	**4**	**5**
C [emu K mol^{-1}]	3.326(5)	2.13(3)	3.111(7)	1.803(1)	1.946(3)
θ [K]	−34.4(4)	−4(2)	−29.0(4)	−2.0(1)	−7.1(2)

in that they suggest the presence of either an $S=3/2$ or $S=5/2$ ground state. In the case of compounds **2**, **4** and **5** (those containing MeCp ligands) the Curie constant of about 1.8–2.1 cm^3 K mol^{-1} is in close agreement with the theoretical value predicted for the $S=3/2$ case (i.e., 1.876 cm^3 K mol^{-1}). Whilst this intermediate $S=3/2$ spin state has been observed in some d^5 iron(III) complexes, to our knowledge this is the first example identified in the isoelectronic Mn^{II} systems.[16]

The cases of compounds **1** and **3**, in which the lack of any MeCp ligands presumably generates a weaker ligand field, are more complex. These do not conform strictly to the isotropic $S=3/2$ case, with Curie constants of 3.326(5) and 3.111(7) cm^3 K mol^{-1}, respectively. These compounds also show much larger Weiss constants, which we ascribe to moderately well-separated energy levels arising from the effect of zero-field splitting rather than exchange coupling.[17] This suggests that the effect of zero-field splitting is more pronounced when the ligand field is smaller. At present we cannot eliminate the possibility of thermal population from an $S=5/2$ excited state, as only very detailed knowledge of the electronic energy levels would allow us to distinguish between these cases.[17]

Experimental Section

General considerations: Manipulations of air-sensitive compounds were carried out under argon by employing standard Schlenk/vacuum-line techniques and a nitrogen-filled glove box containing an atmosphere recirculator equipped with 4 Å molecular sieve and activated copper drying columns. All glassware was dried by heating in vacuo prior to use. THF was pre-dried over sodium wire and was distilled from sodium/benzophenone. Deuterated solvents for NMR spectroscopy were purchased from the Aldrich Chemical Company in sealed ampoules and were used as supplied. Solution-phase ^{1}H NMR spectra were recorded on a Bruker DPX400 NMR spectrometer and were referenced to ^{1}H impurities present in the deuterated solvents. Infrared spectra were recorded on a Perkin–Elmer FT-IR Paragon 1000 Spectrometer as Nujol mulls on NaCl plates. Elemental analyses were performed on an Exeter Analytical CE-440 Elemental Analyser; air-sensitive samples were sealed in pre-weighed, air-tight aluminium boats. Melting points were recorded on a Perkin–Elmer Melting Point Apparatus. Both [(Cp)$_2$Mn] and [(MeCp)$_2$Mn] were synthesised according to literature procedures.[4a,6] Details of the syntheses and characterisations of complex **1** and **3** can be found in reference [9] and will not be repeated here.

Synthesis of 2: A solution of [(Cp)$_2$Mn] (0.37 g, 2.00 mmol) in THF (45 mL) was added to (MeCp)K (0.24 g, 2.00 mmol) at room temperature. The mixture was stirred (2 h), filtered (Celite porosity 3) and reduced in volume until a precipitate formed. The precipitate was re-dissolved and the solution stored at 5 °C (24 h), resulting in the formation of pink crystals of **2**·2 THF. Placing **2**·2 THF under vacuum for approximately 30 min prior to isolation resulted in complete removal of the non-coordinated, lattice THF molecules, yielding **2** (0.13 g, 17 %). Elemental analysis calcd (%) for $C_{20}H_{25}KmnO$: C 64.0, H 6.7; found: C 60.5, H 5.4 %; m.p. 300–315 °C, decomposes to a black solid; IR (Nujol, NaCl): $\tilde{\nu}=$ 3059 (ms; Cp, C–H stretch), 1011 cm^{-1} (ms; THF, C–O stretch); ^{1}H NMR (+25 °C, 400.16 MHz, [D$_8$]THF): $\delta=$6.50 (s), 6.40 (s; Cp$_2$Mn(*thf*), Cp$_2$(MeCp)Mn(*thf*)K), 5.60 (br m; (Me*Cp*)K), 2.92 (m), 2.54 ppm (m; Cp$_2$Mn(*thf*), Cp$_2$(MeCp)Mn(*thf*)K).

Synthesis of 4: A solution of [(Cp)$_2$Mg] (0.15 g, 1.00 mmol) in THF (30 mL) was added to a stirred solution of [(MeCp)$_2$Mn] (0.43 g, 2.00 mmol) in THF (30 mL) at room temperature. The mixture was stirred (1 h) and filtered (Celite, porosity 3), and the pale yellow solution reduced in volume until a precipitate formed. The precipitate was re-dissolved and the solution stored at 5 °C (24 h), resulting in the formation of colourless crystals of **4**·0.5 THF. Placing **4**·0.5 THF under vacuum for approximately 30 min prior to isolation resulted in complete removal of the non-coordinated, lattice THF molecules, yielding **4** (0.40 g, 39 %). Elemental analysis calcd (%) for $C_{58}H_{86}O_6MgMn_2$: C 68.7, H 8.6; found: C 67.6, H 8.5; m.p. 65–67 °C, to a brown oil; IR (Nujol, NaCl): $\tilde{\nu}=$3066 (ms; Cp, C–H stretch), 1012 cm^{-1} (s; THF, C–O stretch); ^{1}H NMR (+25 °C, 400.16 MHz, [D$_8$]THF): $\delta=$ 6.31 (br s; [Cp$_3$Mn(*thf*)]$^-$), 3.52 (m; [Mg(*thf*)$_6$]$^{2+}$), 2.77 (s; *Me*Cp), 1.68 ppm (m; [Mg(*thf*)$_6$]$^{2+}$).

Synthesis of 5: A solution of [(MeCp)$_2$Mn] (0.43 g, 2.00 mmol) in THF (40 mL) was added to a standard solution of [(MeCp)$_2$Mg] in THF (0.25 M, 4.0 mL, 1.00 mmol) at room temperature. The mixture was stirred (1 h) and filtered (Celite, porosity 3), and the pale yellow solution reduced in volume until a precipitate formed. The precipitate was re-dissolved and the solution stored at 5 °C (24 h), resulting in the formation of colourless crystals of [(MeCp)$_3$Mn]$_2$[Mg(thf)$_6$]·0.5 THF. Placing **5**·0.5 THF under vacuum for approximately 30 min results in removal of the lattice-bound THF, yielding **5** (0.54 g, 52 %). Elemental analysis calcd (%) for $C_{60}H_{90}O_6MgMn_2$: C 69.2, H 8.7; found: C 68.2, H 8.2; m.p. 70–72 °C, to a brown oil; IR (Nujol, NaCl): $\tilde{\nu}=$3066 (w; Cp, C–H stretch), 1012 cm^{-1} (m; THF, C–O stretch); ^{1}H NMR (+25 °C, 400.16 MHz, [D$_8$]THF): $\delta=$ 9.35 (br s; [(Me*Cp*)$_3$Mn]$^-$), 6.30 (br s; [(MeCp)$_3$Mn(*thf*)]$^-$), 3.53 (m; [Mg(*thf*)$_6$]$^{2+}$), 2.82 (s; *Me*Cp), 1.68 ppm (m; [Mg(*thf*)$_6$]$^{2+}$).

Synthesis of 6: A solution of [(Cp)$_2$Mn] (0.46 g, 2.50 mmol) in THF (20 mL) was added to a suspension of CpLi (0.09 g, 1.25 mmol) in THF (20 mL) and [12]crown-4 (0.40 mL, 2.50 mmol) at room temperature. The mixture was stirred (1 h) and filtered (celite, porosity 3). The filtrate was

subsequently stored at −15 °C (1 week), resulting in amber coloured crystals of **6** (0.03 g, 1 %).

Magnetic susceptibility measurements: For compounds **1**–**5** magnetic susceptibility measurements were performed on a Quantum Design Magnetic Property Measurement System (MPMS-XL) SQUID magnetometer. Unless otherwise stated, data were collected in an applied field of 700 G, temperature range 5–300 K. Corrections for diamagnetism were made using Pascal's constants. Samples of **1**–**5** were found to be *extremely* air-sensitive and magnetic studies were severely hampered by persistent sample decomposition/degradation. Gelatin capsules were stored in the glove-box for a minimum of 24 h prior to use in order to facilitate removal of trace moisture from the capsule (Prolonged oven-baking tended to make the capsules fragile and inflexible). Samples of **1**–**5** (typically 30–100 mg) were weighed and placed in gelatin capsules in a glove-box. The capsules were then inserted into a straw in the glove box to facilitate mounting in the magnetometer. The capsules were subsequently stored and transferred between glove-box and magnetometer under argon. A short period, typically less than 5 min, was required to introduce the sample into the magnetometer.

X-ray crystallographic studies: X-ray crystallographic data were collected with $Mo_{K\alpha}$ radiation ($\lambda = 0.71069$ Å) on a Nonius KappaCCD (**2**·2 THF, **4**·0.5 THF and **6**) or a Siemens P4 four-circle diffractometer (**5**·0.5 THF), in a low-temperature stream of dinitrogen. Details of data collection and refinement are given in Table 5. Structure solution was by direct methods.[17] In the monoanion of **2**·2 THF the manganese atom lay on an axis of C_3 symmetry (at 0.666, 0.333, 0) bonded in an η^2-mode to one unique cyclopentadienyl ring which was 50:50 disordered, giving two independent rings of half occupancy. Consequently the one methyl carbon atom per monoanion occurred in the crystal randomly disordered over the two sets of three symmetry-related Cp rings, so the two independent sites in the asymmetric unit were each assigned occupancies of 0.16667. The potassium cation also showed 50:50 disorder at two sites (K(1) and K(2)) located on a second C_3 axis (0, 0, z), such that the distances to K(1) were optimised for bonding to the carbon atoms of the first component of the Cp disorder (C(11) to C(15)) and to K(2) for the second (C(21) to C(25)). Two maxima of electron density lying on the second C_3 axis at about 3.0 Å from K(1) and K(2), respectively, were assigned as oxygen atoms O(1) and O(2) of half occupancy (attributed to THF ligands coordinated to the disordered potassium cations). Due to the high site symmetry, the two independent THF half components overlapped and the corresponding carbon atoms were only detected as an extended "spherical" region of residual electron density. Two additional isolated "spherical" regions of electron density were also detected lying across C_3 axes and were interpreted as highly disordered solvated THF molecules. Apart from the two half oxygen atoms coordinated to K(1) and K(2), no individual atom nor any reasonable image could be obtained for any of the three THF units. The most satisfactory refinement was obtained by including localised maxima of electron density, in these regions, as partial oxygen or partial carbon atoms of fixed occupancy in order to generate the correct overall formulation of the THF molecules. The hydrogen atoms of the THF molecules were not included in structure factor calculation, but the positional and displacement parameters of the partial C and O atoms were refined. The extensive disorder in **2** resulted in poor diffraction at high angle and accounts for the relatively high final residuals and esds on all parameters. Despite this the salient features of the complex are clearly established. The crystals of **4**·0.5 THF and **5**·0.5 THF are apparently isomorphous, the unit cell half of each has a very disordered THF solvent molecule (overall of half occupancy) per $[Mg(thf)_6]^{2+}$ ion, which is not observed in **4**·0.5 THF. The solvent atoms were treated as described above for the structure of **2**·2 THF. In each of the structures, **4**·0.5 THF and **5**·0.5 THF, the manganese atom is on a C_3 axis and the Mg atom is on a site of $\bar{3}$ symmetry. In the $[Cp(MeCp)_2Mn]^-$ ion of **2**·2 THF the two MeCp rings are disordered with the unsubstituted Cp ring over the three symmetry-related positions so that one unique η^2-ring occurs in the asymmetric unit. Therefore at the methyl group site in the asymmetric unit, a methyl group occupancy of 0.66667 and a hydrogen atom of occupancy 0.33333 were assigned, with the bond length of the two components appropriately constrained. The remaining ring hydrogen atoms in **4**·0.5 THF and **5**·0.5 THF were directly located and their parameters refined. Anisotropic displacement parameters were assigned to all full occupancy non-hydrogen atoms in **2**·2 THF, **4**·0.5 THF and **5**·0.5 THF, and the refinement was by full-matrix least squares on F^2.[18]

Acknowledgements

The authors would like to thank Dr. J. E. Davies (Cambridge) for collecting the X-ray diffraction data on compounds **2**·2 THF, **4**·0.5 THF and **5**·0.5 THF. For financial assistance the authors would like to thank the EPSRC (C.S.A, R.A. L., M.McP., R.A.M., J.M.R., P.T.W., D.S.W.), The Isaac Newton Trust (R.A.L.) and Electron Industries, UK, Ltd. (R.A.L.). R.A.L. would also like to thank Clare College, Cambridge, for the award of the Denman Baynes Research Fellowship.

[1] J. P. Collman, L. Hegedus, *Principles and Applications of Organotransition Metal Chemistry*, University Science Books, Oxford, **1980**, Chapter 2, p. 13.
[2] a) P. H. M. Budzelaar, J. J. Engelberts, J. H. van Lenthe, *Organometallics* **2003**, *22*, 1562; b) P. Jutzi, N. Burford, *Chem. Rev.* **1999**, *99*, 969; c) M. A. Beswick, J. S. Palmer, D. S. Wright, *Chem. Soc. Rev.* **1998**, *27*, 225.
[3] N. J. Long, *Metallocenes; An Introduction to Sandwich Complexes*. Blackwell Science, Oxford, **1998**.
[4] a) G. Wilkinson, F. A. Cotton, J. M. Birmingham, *J. Inorg. Nucl. Chem.* **1956**, *2*, 95; b) E. König, V. P. Desai, B. Kanellakopoulos, R. Klenze, *Chem. Phys.* **1980**, *54*, 109.
[5] a) H. Mutoh, S. J. Masuda, *J. Chem. Soc. Dalton Trans.* **2002**, 1875; b) S. Evans, M. L. H. Green, B. Jewitt, G. H. King, A. F. Orchard, *J. Chem. Soc. Faraday Trans. 2* **1974**, *70*, 356; c) M. E. Switzer, M. F. Rettig, *J. Chem. Soc. Chem. Commun.* **1972**, 687; d) A. Haaland, *Inorg. Nucl. Chem. Lett.* **1979**, *15*, 267.
[6] L. T. Reynolds, G. Wilkinson, *J. Inorg. Nucl. Chem.* **1959**, *9*, 86.
[7] a) M. E. Switzer, R. Wang, M. F. Rettig, A. H. Maki, *J. Am. Chem. Soc.* **1974**, *96*, 7669; b) J. H. Ammeter, R. Bucher, N. Oswald, *J. Am. Chem. Soc.* **1974**, *96*, 7833; c) A. Almenningen, A. Haaland, S. Samdal, *J. Organomet. Chem.* **1978**, *149*, 219.
[8] S. Harder, *Angew. Chem.* **1998**, *110*, 1357; *Angew. Chem. Int. Ed.* **1998**, *37*, 1239; S. Harder, M. H. Prosenc, *Angew. Chem.* **1994**, *106*, 1830; *Angew. Chem. Int. Ed. Engl.* **1994**, *33*, 1744; S. Harder, M. H. Prosenc, *Angew. Chem.* **1996**, *108*, 101; *Angew. Chem. Int. Ed. Engl.* **1996**, *35*, 97; S. Harder, *Coord. Chem. Rev.* **1998**, *176*, 17.
[9] A. D. Bond, R. A. Layfield, J. A. MacAllister, M. McPartlin, J. M. Rawson, D. S. Wright, *Chem. Commun.* **2001**, 1956.
[10] S. Kheradmandan, H. W. Schmalle, H. Jacobsen, O. Blacque, T. Fox, H. Berke, M. Gross, S. Decurtins, *Chem. Eur. J.* **2002**, *8*, 2526.
[11] M. J. Duer, N. A. Page, M. A. Paver, P. R. Raithby, M.-A. Rennie, C. A. Russell, C. Stourton, A. Steiner, D. S. Wright, *J. Chem. Soc. Chem. Commun.* **1995**, 1141; M. A. Beswick, H. Gornitzka, J. Kärcher, M. E. G. Mosquera, J. Palmer, P. R. Raithby, C. A. Russell, D. Stalke, A. Steiner, D. S. Wright, *Organometallics* **1999**, *18*, 1148.
[12] H. Sitzmann, *Coord. Chem. Rev.* **2001**, *214*, 287.
[13] A precedent for this has recently been reported in the case of polymorphs of $[(Cp)_2Pb]$: C. A. Morrison, R. A. Layfield, D. S. Wright, *J. Am. Chem. Soc.* **2002**, *124*, 6775.
[14] R. Krieger, J. Voitlander, *Z. Naturforsch. A* **1972**, *27*, 1082; J. Voitlander, E. Schimitschek, *Z. Elektrochem.* **1957**, *61*, 941.
[15] R. L. Carlin, *Magnetochemistry*, Springer, Berlin, **1986**.
[16] See for example the dithiocarbamate salts of Fe^{II}; H. H. Wickman, *J. Chem. Phys.* **1972**, *56*, 976.
[17] O. Kahn, *Molecular Magnetism*, VCH, Weinheim, **1993**.
[18] G. M. Sheldrick, SHELX-97, University of Göttingen, Göttingen, Germany, **1997**.

Received: October 4, 2005
Published online: February 2, 2006

